

# Extreme Wind Speed Modeling across Garoua City and Implications Assessing for the Flight Activities

Daïka Augustin<sup>1,2\*</sup>, Mbane Biouele Cesar<sup>2</sup>

<sup>1</sup>Department of Meteorology and Climatology, National Advanced School of Engineering, University of Maroua, Maroua, Cameroon

<sup>2</sup>Laboratory of Earth's Atmosphere Physics, Faculty of Science, University of Yaoundé 1, Yaoundé, Cameroon

Email: \*augustindaika@yahoo.fr

**How to cite this paper:** Augustin, D. and Cesar, M.B. (2025) Extreme Wind Speed Modeling across Garoua City and Implications Assessing for the Flight Activities. *Atmospheric and Climate Sciences*, 15, 696-708.

<https://doi.org/10.4236/acs.2025.153035>

**Received:** April 2, 2025

**Accepted:** July 27, 2025

**Published:** July 30, 2025

Copyright © 2025 by author(s) and Scientific Research Publishing Inc. This work is licensed under the Creative Commons Attribution International License (CC BY 4.0).

<http://creativecommons.org/licenses/by/4.0/>



Open Access

---

## Abstract

In this paper, we analyze the directions, intensities, spatial and temporal distributions, variability, and trends of extreme wind events using wind speed data that span between the 2012-2017 periods in Garoua City. The results obtained show that the wind blows a little almost from all directions and the dominant direction is from the North-West with more than 40% of winds in this direction, the dominant axis is SE-NW with more than 55% of winds in this axis and the annual mean wind speed at a height of 10 m is 5 m/s in 2014. It was further shown that it decreased until it was canceled in 2017 characteristic of the calm wind. In this context, the forecast of the wind speed variability (intensities and directions) becomes very crucial. This fact denotes a problem for lighter aircraft, whose crosswind rates are lower.

## Keywords

Extreme Wind Events, Garoua City, Wind Speed Variability

---

## 1. Introduction

The wind is an important weather parameter for aeronautics during taxiing, take-off, landing, navigation [1] [2], and safety in the air [3], for urbanization during the dispersion or concentration of pollutants around industrial sites or in cities [4] [5], for agronomy during certain sensitive crops [6] [7] and for renewable energy during the production and evaluation of wind energy potential [8]-[13]. In addition, the force released by the wind can also be experienced as a major climatic constraint [14]-[17], capable of causing considerable damage to the most solid infrastructures [18], or even weakening certain economic sectors of one or even

several countries simultaneously [19].

The implications presented above highlight the need to model this phenomenon and understand the physical processes responsible for their prediction. Its modeling has been the subject of much work in recent years. Wind speed Variations allow us to understand the climate change effect in the area of interest, especially since its impact on wind speed differs considerably from one place to another [15]. Although these variations are essential to the environment, their assessment in Cameroon, particularly in Garoua City, has been ignored or non-existent, or also not well understood. The lack of literature on future spatiotemporal variations of wind speed is particularly apparent in this area.

Several analytical studies [20]-[24] have noted that a Rayleigh distribution (a special case of the Weibull distribution) emerges for the wind speed if its components are assumed to be individually Gaussian. To obtain a physical understanding of the observed Probability Distribution Functions (PDF) of sea surface wind speeds, a stochastic model for boundary layer winds (including several assumptions and parameterizations) was developed [25].

The motivation for this work is to know the local weather conditions and improve forecasts for Garoua City. To achieve our objective, data from pilot probes and synoptic observation stations recorded during the period 2012-2017 have been used to numerically analyze the spatiotemporal variability of the wind likely to attenuate activities in the Sahelo-Sudanian zones and in particular the Garoua city based on the hydrodynamic model. The latter reflects the behavior of the speed module, as this value is used in statistical studies. In addition to the statistical approach, a description of the probability distribution of observed wind speed was based on theoretical ideas drawn from the hydrodynamic peculiarities of atmospheric motion. This is justified by studying the products of numerical simulations or the equations sufficiently simplified to obtain their analytical solutions.

The data used and methodology are described in Section 2. The results and discussions are given in Section 3. The conclusion is drawn in Section 4.

## 2. Data Used and Methodology

### 2.1. Study Zone

Garoua is the capital of the Northern Cameroon Region which extends between 8° and 10° north latitude and between 12° and 16° east longitude. This region is located to the North by the Far North region, to the South by the Adamawa region, to the East by the Republic of Chad and the Central African Republic, to the West by the Federal Republic of Nigeria (Figure 1). Its climate is Sudano-Sahelian, characterized by a dry season and a rainy season [26]. It is strongly influenced by the presence of the Bénoué River and the Mayo Kébi, Lébri, Badjouma, and Bangaï. Data from the Garoua airport rainfall station show an average annual rainfall of 1200 mm and an annual average temperature of around 25°C.

Its relief is generally rugged and is made up of a mountainous area (Mont Tinguélin) and the valley (Bénoué valley). The hydrographic network is made up of a

few rivers. The soils are strongly eroded sedimentary and clayey types.

### 2.2. Data Used

The data used was collected by the VANTAGE PRO system at the observation station at Garoua aerodrome. It is located 2.1 NM NNW of downtown Garoua and is oriented East/West (more precisely 890/2690). The references for Garoua aerodrome are given in **Table 1**. They are available 24 hours a day and every day. These data were processed using the R statistical processing software [27]-[30].

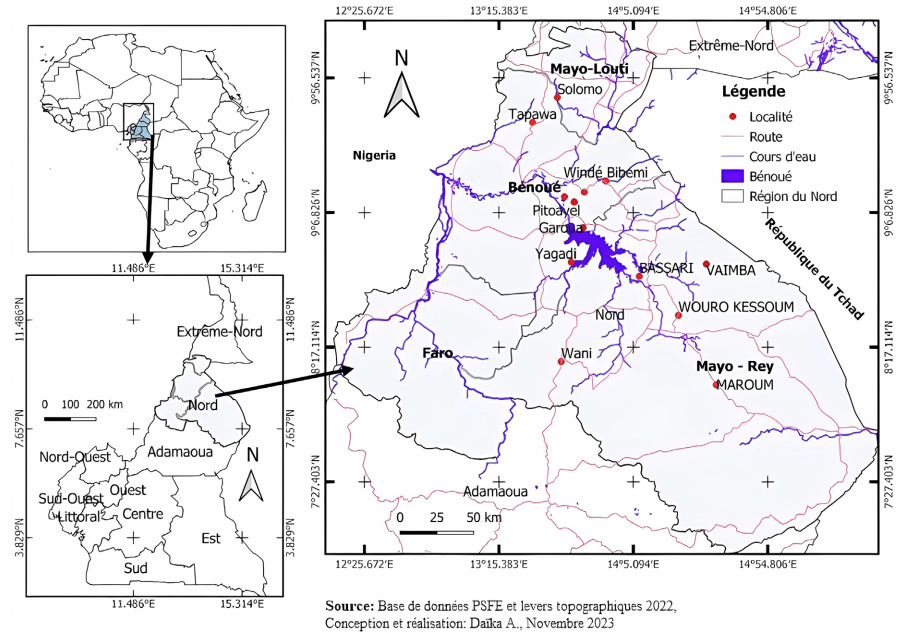


**Figure 1.** Locations of the climatological observing stations for which the data set has observation records.

**Table 1.** Table giving the references of the Garoua aerodrome.

ICAO Location Indicator	FKKR
Track length	3450 m
Track width	45 m
Track orientation	E/W (89° and 269°)
Airfield altitude	242 m
Latitude	09° 20'12"N
Longitude	013° 22'52"E
Location of weather parameter measurement sensors	Glide path (touchdown zone RWY09)

### 2.3. Methodological Approach

We consider the hydrodynamic model following that reflects the behavior of the

velocity modulus, to physically understand the simulated PDFs of surface wind speeds.

According to the equation of motion, the acceleration of the horizontal velocity vector is given by:

$$\frac{d\mathbf{u}_h}{dt} = -\nabla_p \Phi - f \mathbf{k} \wedge \mathbf{u}_h \quad (1)$$

where  $\mathbf{u}_h$  the horizontal velocity vector,  $\nabla_p$  the horizontal gradient operator applied with pressure held constant,  $\Phi$  geopotential and  $f$  the Coriolis parameter.

It is simpler to use natural coordinates to investigate the acceleration of the horizontal velocity vector in curves [31].

In the natural coordinate system,  $\hat{s}$  follows the flow,  $\hat{n}$  is normal to the flow and to the left of  $\hat{s}$ , and  $\hat{k}$  is vertical.

Then, Equation (1) can be expanded in the natural coordinate system and we obtain the following component equations:

$$\frac{dU}{dt} = -\frac{\partial \Phi}{\partial s} \quad (2)$$

And

$$\frac{U^2}{R} = -\frac{\partial \Phi}{\partial n} - fU \quad (3)$$

Equation (3) is transformed to obtain equation (4):

$$\frac{U^2}{Rf} + U = U_g \quad (4)$$

with  $U_g$  is the geostrophic wind and is defined as  $U_g = -\frac{1}{f} \frac{\partial \Phi}{\partial n}$ , and  $R$  is the curvature radius.

Equation (4) can be used to calculate the wind speed Probability Distribution Function by knowing the geostrophic wind Probability Distribution Function [24].

Thus, the expression for the wind speed Probability Distribution Function and Cumulative Distribution Function is given respectively by:

$$g(U) = \left( \frac{2U}{Rf} + 1 \right) \frac{1}{2\sigma_g \sqrt{\pi\chi}} \exp(-\Psi(U)) \quad (5)$$

And

$$G(U) = \frac{1}{2} \left[ 1 + \operatorname{erf} \left( \sqrt{\Psi(U)} \right) \right] \quad (6)$$

$$\text{with } \Psi(U) = \frac{\left( \frac{U^2}{Rf} + U \right)^2}{4\sigma_g^2 \chi}.$$

where  $\sigma_g$  standard deviation of the geostrophic wind and  $\chi = 1 - \eta$ ,  $\eta$  the autocorrelation coefficient between height fluctuations at point "1" and "2".

In the following, we numerically investigate the extreme wind speed across Garoua city. The curves are performed by R and MATLAB programs. With the MATLAB program, we chose 1000 iterations that produce figures with relevant color coding.

### 3. Results and Discussions

#### 3.1. Distribution of Wind Speed Direction over 2012-2017 Period

**Figure 2** displays the wind speed direction rose diagrams over 2012-2017 period. It provide useful information on the distribution of wind direction and availability of directional wind speed. The wind rose constructed using measurements of the wind speeds and corresponding wind directions. The blue portion represents the wind speed  $< 1$  m/s. The green portion shows the wind speed at 1 - 2 m/s; the orange yellow portion indicates that the wind speed is 2 - 3 m/s; the brown portion indicates that the wind speed has exceeded 3 - 13.4 m/s. Occurrence distribution of wind speed and direction for the annual average has been observed. According to **Figure 2**, the wind varies in all directions and the dominant direction is North-West with more than 40% of winds in this direction, and the dominant axis is SE-NW with more than 55% of wind direction in this axis.

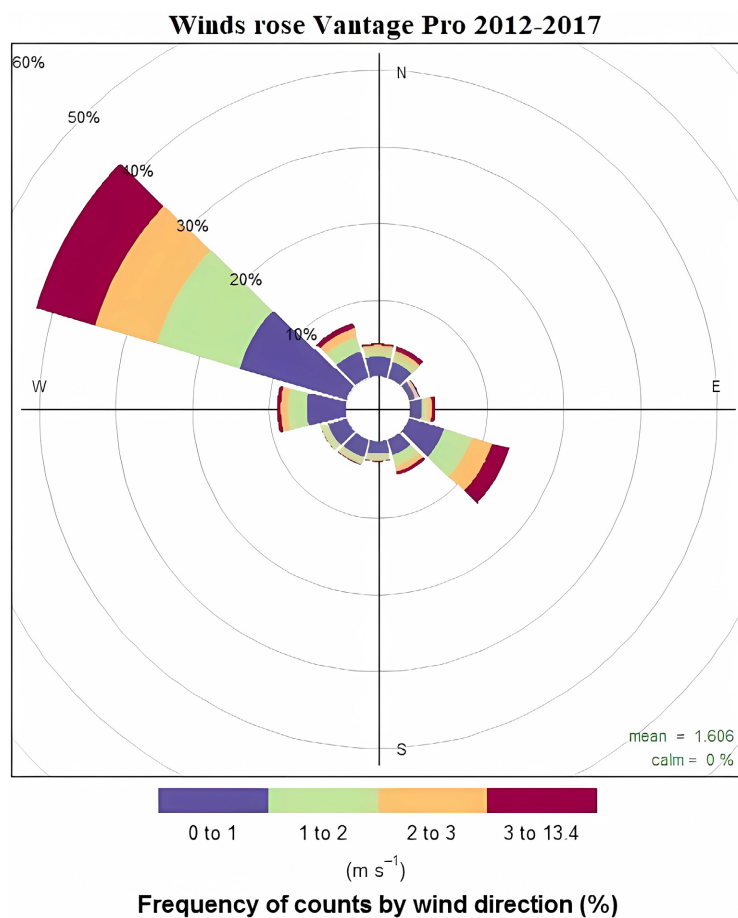


**Figure 2.** Wind speed direction rose diagrams over 2012-2017 period.

**Figure 3** illustrates the wind direction boxplots for each month of the period 2012-2017. We observe that the value of the median wind direction at the Garoua station is  $140^\circ$  in the months of January and February; hence the wind direction is SE,  $250^\circ$  in the month of March showing a WSW direction,  $290^\circ$  in the months of April, May, June, and July indicating the WNW direction and reaches a maximum of  $320^\circ$  proving the wind is from the NW in August. We also note that during the months of September and October, the median wind direction is  $290^\circ$  from a WNW direction. The wind is  $210^\circ$  SSW in November and  $150^\circ$  SSE in December. The largest value recorded is  $340^\circ$  NNW direction. The wind turns clockwise from January to August and from the SE sector to the NNW sector, it then returns counterclockwise from August to January. This proves the wind speed variability in this region. In **Figure 3**, the coherence of extremal behavior across directions suggests that direction could be treated as a covariate of the parameters in the distribution of the statistics [21].

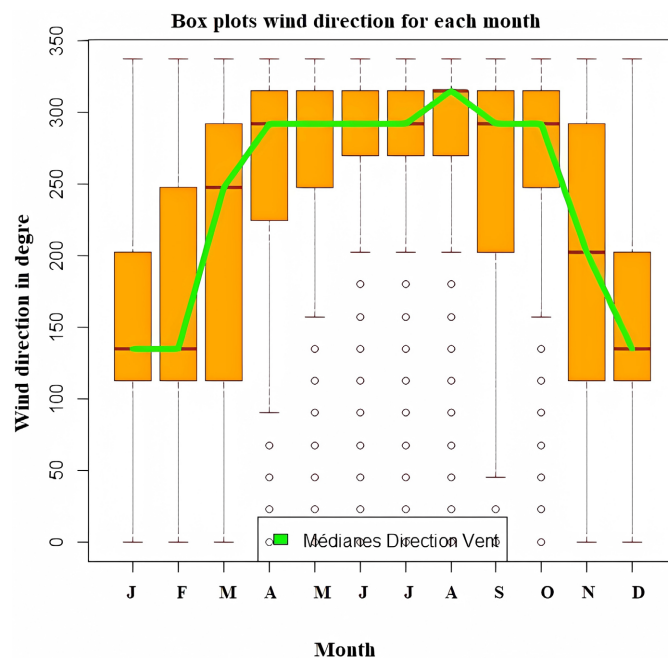


**Figure 3.** Monthly distribution of wind speed direction over the 2012-2017 period.

**Figure 4** displays the wind direction boxplots for each year. It shows that the annual distribution is asymmetrical and the distribution is more elongated towards the largest values. The dominant wind direction is WSW ( $250^\circ$ ) in 2012, the wind has a dominant direction of WNW ( $300^\circ$ ) from 2013 to 2015 and it is  $290^\circ$  characteristic of the dominant WNW wind direction.

### 3.2. Distribution of Wind Speed Intensities Over 2012-2017 Period

**Figure 5** illustrates the boxplots of wind speed intensities for each month in Garoua City. According to **Figure 5**, the lower horizontal line of each boxplot represents the first quartile (Q1), that is, the middle number between the smallest and

the median of the wind speed dataset. The yellow part represents the interquartile range (IQR), that is, the 25th to the 75th percentile. The horizontal line in the IQR represents the median of the dataset. The upper horizontal line shows the Q3. All datasets shown outside the boxplots are outliers.

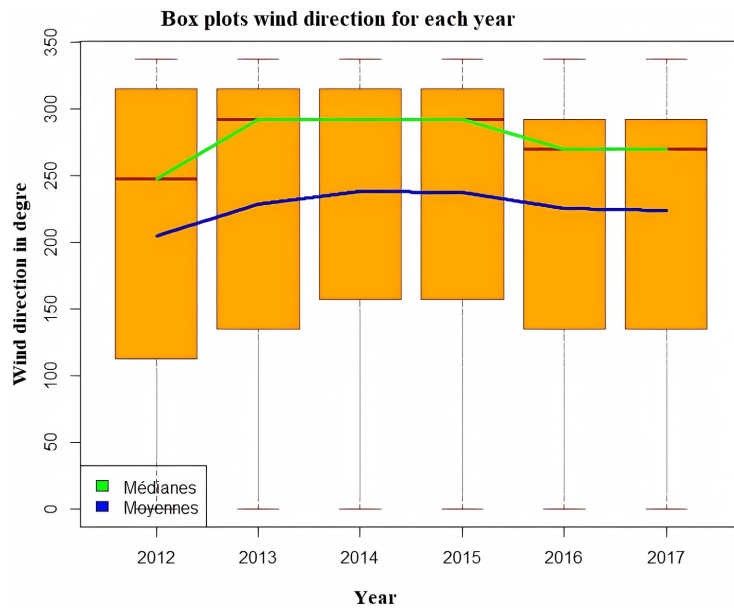


**Figure 4.** Annual distribution of wind speed direction over 2012-2017 period.

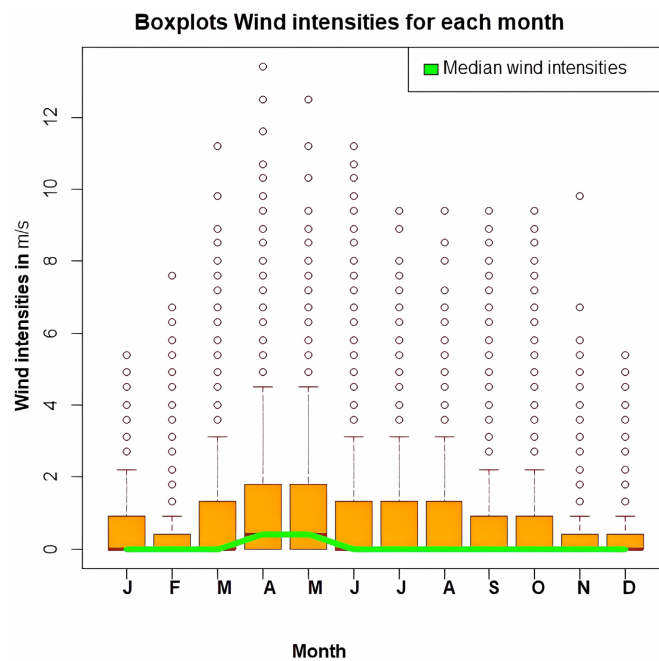


**Figure 5.** Monthly distribution of wind speed intensities Across Garoua based on data from surface wind observing stations for the period 2012-2017.

Further, Results indicate that with average near-surface wind speeds of 0.4 m/s, a minimum of 0 m/s, and a maximum of 5 m/s, winds are rarely strong in Garoua

(Figure 5). The maximum wind speed was observed in April and May, with an extreme value above 12 m/s in April, while the minimum was reported in January, February, March, June, July, August, September, October, November, and December. It is notable however that calm conditions generally exist across the region, and this can be attributed to the Sahel-sudanese climate with prevailing trade winds within the Hadley circulation [32] [33].

Figure 6 represents a box plot of wind intensities for each year in Garoua City during the 2012-2017 period. In Figure 6, we see an increase in the average wind speed, going from 3 m/s to 5 m/s, and that a decrease in the average wind speed, going from 5 m/s to 0 m/s. Thus, we observe that a maximum of the average of the wind speed values in 2014 and the year where we observed the greatest value which is 5 m/s, then it decreases until it disappears in 2017 calm wind characteristic. We conclude that the speed will be canceled out over time.

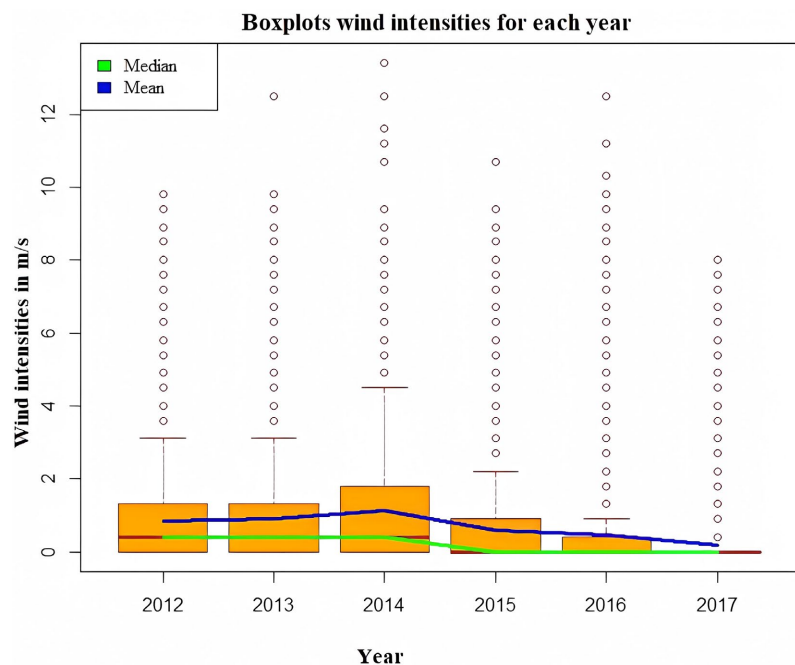
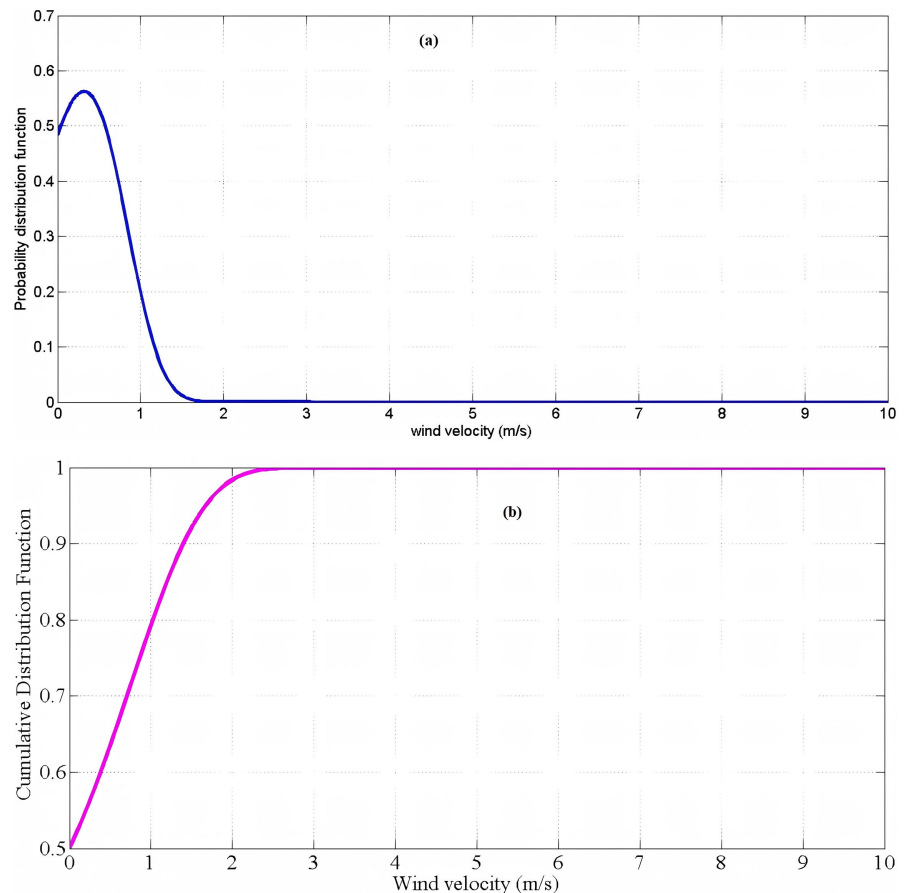


Figure 6. Annual distribution of wind speed intensities over the 2012-2017 period.

Figure 7 displays the probability density function and Cumulative density function of the monthly distribution of maximal wind speed intensities for the study zone using the hydrodynamic model. It is obtained in using the equations (5) and (6) respectively with  $Rf = 2281$  and  $\rho = 0.0346$ . The curves resemble the Weibull distribution. The probability density function is used to illustrate the fraction of time for which a given wind speed possibly prevails at a region. We observe that the peak of the density function frequencies of all the sites skewed towards the higher values of mean wind speed (Figure 7(a)). It should be remarked that the peak of the probability density function curve indicates the most frequent velocity. It can be observed from Figure 7(a) that the most frequent wind speed expected is 0.4 m/s.

The cumulative distribution function (**Figure 7(b)**) can be used to estimate the time for which wind speed is within a certain speed interval. For wind speeds greater or equal to 2 m/s cut-in wind speed, it has frequencies of about 98% while the same location has frequencies of about 65% for wind speed of 0.5m/s cut-in wind speed. In short, the frequency is greater than 50 % for any wind speed. The saturation level for the cumulative distribution function is at about 2 - 3 m/s.



**Figure 7.** Monthly distribution of maximal wind speed intensities: (a) Probability density function and (b) Cumulative density function.

**Figure 8** exhibits the probability density function and Cumulative density function of the monthly distribution of extreme wind speed intensities for the study zone using the hydrodynamic model. The saturation level for the cumulative distribution function is at about 3, 6 m/s. We see that **Figure 8** has the same appearance as **Figure 7** but the value of the extrema is different (0.56 for **Figure 7(a)** and 0.32 for **Figure 8(a)**) and does not have the same saturation level.

The airport is sometimes subject to the convective systems action, the West African monsoon, and geographical discontinuities (different heating depending on the nature of the ground, relief effects, etc.) due to its geographical position.

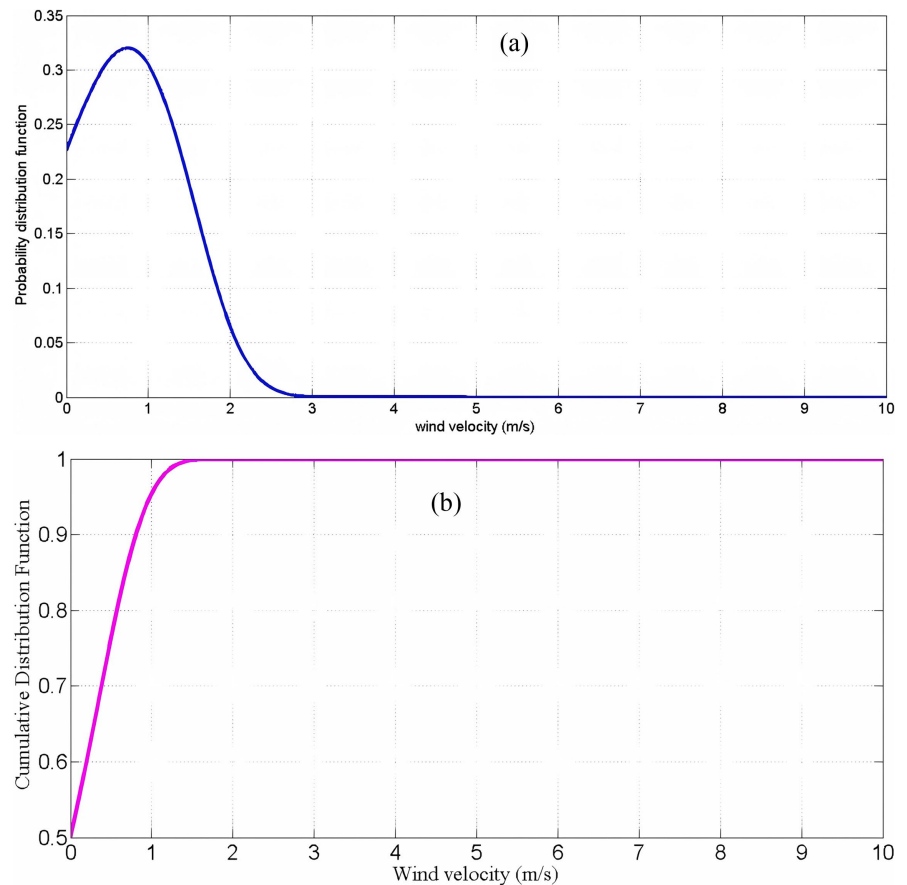


**Figure 8.** Monthly distribution of extreme wind speed intensities: (a) Probability density function and (b) Cumulative density function.

#### 4. Conclusion

This work focuses on the analysis of the directions, intensities, spatial and temporal distributions, variability, and trends of extreme wind events using wind speed data that span between the 2012-2017 period and measured at a height of 10 m, using the R and MATLAB programs. The results obtained show that the distribution function has a form close to that of the Weibull distribution. This demonstrates the bridge between hydrodynamics and extreme event statistics. In Garoua airport, the wind blows a little from almost all directions and the dominant direction is from the North-West with more than 40% of winds in this direction, the axis dominant is SE-NW with more than 55% of winds and the average annual wind speed at a height of 10 m is 5 m/s in 2014. In addition, it decreased until it disappeared in 2017, characteristic of calm wind. Therefore, forecasting variabilities or changes in wind intensity and direction is crucial for good management of activities in Garoua city and in this airport in particular, especially when they occur abruptly and the wind speed is high. This overspeed is due to the thermobaric contrast during and after the passage of the cold front and to the superposition of the jet stream on the cold front. It results in the formation of a dynamic tropopause anomaly that determines the intensification of microclimate instability.

## Acknowledgements

The authors are grateful to all referees for their valuable suggestions.

## Conflicts of Interest

The authors declare no conflicts of interest regarding the publication of this paper.

## References

- [1] Augustin, D., Pascal, I.M., Oumarou, M.M. and Cesar, M.B. (2022) Analysis of Weather Conditions for Aerial Security and Optimization in Maroua-Salak. *Atmospheric and Climate Sciences*, **12**, 172-188. <https://doi.org/10.4236/acs.2022.121012>
- [2] O'Connor, A. and Kearney, D. (2019) Low Level Turbulence Detection for Airports. *International Journal of Aviation, Aeronautics, and Aerospace*, **6**, Article No. 3. <https://doi.org/10.15394/ijaaa.2019.1302>
- [3] Augustin, D. and Cesar, M.B. (2022) Analysis of Wind Shear Variability and Its Effects on the Flights Activities at the Garoua Airport. *Journal of Extreme Events*, **9**, Article ID: 2250006. <https://doi.org/10.1142/s2345737622500063>
- [4] Kastendeuch, P.P. and Kaufmann, P. (1997) Classification of Summer Wind Fields over Complex Terrain. *International Journal of Climatology*, **17**, 521-534. [https://doi.org/10.1002/\(sici\)1097-0088\(199704\)17:5<521::aid-joc143>3.0.co;2-q](https://doi.org/10.1002/(sici)1097-0088(199704)17:5<521::aid-joc143>3.0.co;2-q)
- [5] Daïka A. (2024) Investigating the Viscosity and Surfactant Effect on Gravity Waves in the Ocean. *Çankaya University Journal of Science and Engineering*, **21**, 6-17.
- [6] Azad, A., Rasul, M. and Yusaf, T. (2014) Statistical Diagnosis of the Best Weibull Methods for Wind Power Assessment for Agricultural Applications. *Energies*, **7**, 3056-3085. <https://doi.org/10.3390/en7053056>
- [7] Beltrando, G. (1998) Les gelées printanières en champagne viticole: Quelques résultats obtenus à partir d'un nouveau réseau de stations automatiques. *La Météorologie*, **8**, 30-43. <https://doi.org/10.4267/2042/47040>
- [8] Akpınar, S. and Akpınar, E.K. (2009) Estimation of Wind Energy Potential Using Finite Mixture Distribution Models. *Energy Conversion and Management*, **50**, 877-884. <https://doi.org/10.1016/j.enconman.2009.01.007>
- [9] Brigadier, L. and Heiko, P. (2022) Modelling Wind Speed across Zambia: Implications for Wind Energy. *International Journal of Climatology*, **43**, 772-786.
- [10] Kidmo, D.K., Danwe, R., Doka, S.Y. and Djongyang, N. (2015) Statistical Analysis of Wind Speed Distribution Based on Six Weibull Methods for Wind Power Evaluation in Garoua, Cameroon. *Revue des Energies Renouvelables*, **18**, 105-125.
- [11] Wang, Z. and Liu, W. (2021) Wind Energy Potential Assessment Based on Wind Speed, Its Direction and Power Data. *Scientific Reports*, **11**, Article No. 16879. <https://doi.org/10.1038/s41598-021-96376-7>
- [12] Sunday, O.O., Muyiwa, S.A. and Samuel, S.P. (2012) Analysis of Wind Speed Data and Wind Energy Potential in Three Selected Locations in South-East Nigeria. *International Journal of Energy and Environmental Engineering*, **3**, Article No. 7. <http://www.journal-ijeee.com/content/3/1/7>
- [13] Tchinda, R. and Kaptoum, E. (2003) Wind Energy in Adamaoua and North Cameroon Provinces. *Energy Conversion and Management*, **44**, 845-857. [https://doi.org/10.1016/s0196-8904\(02\)00092-4](https://doi.org/10.1016/s0196-8904(02)00092-4)
- [14] Augustin, D., Pascal, I.M., Honoré, M.E. and Cesar, M.B. (2023) Impact of Extreme Rainfall Variability and Changes on Ground Traffic in Cameroon. *Theoretical and*

- Applied Climatology*, **155**, 3175-3185. <https://doi.org/10.1007/s00704-023-04801-w>
- [15] Davy, R., Gnatiuk, N., Pettersson, L. and Bobylev, L. (2018) Climate Change Impacts on Wind Energy Potential in the European Domain with a Focus on the Black Sea. *Renewable and Sustainable Energy Reviews*, **81**, 1652-1659. <https://doi.org/10.1016/j.rser.2017.05.253>
- [16] Sawadogo, W., Abiodun, B.J. and Okogbue, E.C. (2019) Projected Changes in Wind Energy Potential over West Africa under the Global Warming of 1.5°C and Above. *Theoretical and Applied Climatology*, **138**, 321-333. <https://doi.org/10.1007/s00704-019-02826-8>
- [17] Schaeffer, R., Szklo, A.S., Pereira de Lucena, A.F., Moreira Cesar Borba, B.S., Pupo Nogueira, L.P., Fleming, F.P., *et al.* (2012) Energy Sector Vulnerability to Climate Change: A Review. *Energy*, **38**, 1-12. <https://doi.org/10.1016/j.energy.2011.11.056>
- [18] Sarkodie, S.A. and Adams, S. (2020) Electricity Access and Income Inequality in South Africa: Evidence from Bayesian and NARDL Analyses. *Energy Strategy Reviews*, **29**, Article ID: 100480. <https://doi.org/10.1016/j.esr.2020.100480>
- [19] Jung, C. and Schindler, D. (2021) The Role of the Power Law Exponent in Wind Energy Assessment: A Global Analysis. *International Journal of Energy Research*, **45**, 8484-8496. <https://doi.org/10.1002/er.6382>
- [20] Chen, H., Birkelund, Y., Anfinsen, S.N., Staupe-Delgado, R. and Yuan, F. (2021) Assessing Probabilistic Modelling for Wind Speed from Numerical Weather Prediction Model and Observation in the Arctic. *Scientific Reports*, **11**, Article No. 7613.
- [21] Coles, S.G. and Walshaw, D. (1994) Directional Modelling of Extreme Wind Speeds. *Applied Statistics*, **43**, 139-157. <https://doi.org/10.2307/2986118>
- [22] Meissner, T., Smith, D. and Wentz, F. (2001) A 10 Year Intercomparison between Collocated Special Sensor Microwave Imager Oceanic Surface Wind Speed Retrievals and Global Analyses. *Journal of Geophysical Research: Oceans*, **106**, 11731-11742. <https://doi.org/10.1029/1999jc000098>
- [23] Wais, P. (2017) A Review of Weibull Functions in Wind Sector. *Renewable and Sustainable Energy Reviews*, **70**, 1099-1107. <https://doi.org/10.1016/j.rser.2016.12.014>
- [24] Kislov, A. and Matveeva, T. (2021) Extreme Values of Wind Speed over the Kara Sea Based on the ERA5 Dataset. *Atmospheric and Climate Sciences*, **11**, 98-113. <https://doi.org/10.4236/acs.2021.111007>
- [25] Monahan, A.H. (2006) The Probability Distribution of Sea Surface Wind Speeds. Part I: Theory and Seawinds Observations. *Journal of Climate*, **19**, 497-520. <https://doi.org/10.1175/jcli3640.1>
- [26] Augustin, D., Pascal, I.M., Jores, T.K., Elisabeth, F.D., Cesar, M.B., Michael, T.F., *et al.* (2023) Impact Assessment of the West African Monsoon on Convective Precipitations over the Far North Region of Cameroon. *Advances in Space Research*, **72**, 666-676. <https://doi.org/10.1016/j.asr.2022.04.044>
- [27] Galit, S. and Kenneth Jr., C.L. (2016) Practical Time Series Forecasting with R: A Hands-On Guide. 2nd Edition, Axelrod Schnell.
- [28] Ihaka, R. and Gentleman, R. (1996) R: A Language for Data Analysis and Graphics. *Journal of Computational and Graphical Statistics*, **5**, 299-314. <https://doi.org/10.1080/10618600.1996.10474713>
- [29] Lafaye de Micheaux, P., Drouilhet, R. and Lique, B. (2011) Le logiciel R, Maîtriser le langage, Effectuer des analyses statistiques. Springer-Verlag.
- [30] Wayne, A.W., Gray, H.L. and Elliott, A.C. (2017) Applied Time Series Analysis, with R. 2nd Edition, Taylor & Francis, 752.

- [31] Holton, J.R. and Hakim, G.J. (2013) An Introduction to Dynamic Meteorology. 5th Edition, Academic Press, 552. <https://doi.org/10.1016/C2009-0-63394-8>
- [32] Freychet, N., Hegerl, G., Mitchell, D. and Collins, M. (2021) Future Changes in the Frequency of Temperature Extremes May Be Underestimated in Tropical and Sub-tropical Regions. *Communications Earth & Environment*, **2**, Article No. 28. <https://doi.org/10.1038/s43247-021-00094-x>
- [33] Mbane, B.C. (2015) Earth's Atmosphere Dynamic Balance Meteorology. Scientific Research Publishing Inc., 110.